Long Non-coding RNA PTCSC3 Promotes Apoptosis of Human Papillary Thyroid Carcinomas by Regulating S100A4

Qiong Wu
Huaian City Second People's Hospital
Liang Jiang
Qingdao Women and Childrens Hospital
Jiang Wu
Huaian City Second People's Hospital
HaiFang Dong
Huaian City Second People's Hospital
Yaping Zhao (ypzgaochun@163.com)
Nanjing Gaochun People's Hospital https://orcid.org/0000-0002-3408-1545

Research article

Keywords: PTCSC3, S100A4, thyroid carcinoma, subcutaneous xenograft, angiogenesis

Posted Date: May 12th, 2020

DOI: https://doi.org/10.21203/rs.3.rs-26679/v1

Abstract

Objective: We investigated the effect of papillary thyroid carcinoma susceptibility candidate 3 (PTCSC3) on the apoptosis of human papillary thyroid carcinomas cells by regulating S100A4.

Methods: Normal cells Nthy-ori 3-1, cancer cells SW579 and TPC-1 were used to study. Proliferation of human papillary thyroid carcinomas cells was detected by CCK8, clone formation and transwell. Tube formation assay was used to observe the formation of in vitro tubes. Western blot was applied to detect the expressions of S100A4. After S100A4 overexpressed or down expressed, the above experiments were repeated. Tumor volume and weight was measured. Ki67 expression and tumor microvascular density (MVD) were detected by immunohistochemistry. Apoptosis of tissues was detected by TUNEL. Expression of apoptosis-related proteins, VEGF and MMP-9 were detected.

Results: PTCSC3 overexpression and S100A4 lowexpression had significantly decreased proliferation, invasion, migration and tube formation of cancer cells. Meanwhil, the expression of Ki67 and MVD in tumor tissues were significantly decreased ($p<0.05$).

Conclusion: Up-regulation of PTCSC3 can inhibit the expression of S10044, and promoted cell apoptosis and tube formation of papillary thyroid carcinomas cells.

1. Introduction

In the past few decades, patients with papillary thyroid carcinomas have increased rapidly [(1)] and papillary thyroid carcinomas (PTC) account for about 80% - 85% of all thyroid carcinomas [(2)]. The survival rate of PTC can decrease drastically due to distant metastases. Long non-coding RNA (lncRNA) is a non-protein-encoding RNA molecule of more than 200 nucleotides in length. Studies have shown that lncRNA is related to many biological processes, including the development and immunity of cell, cell proliferation and differentiation, modulation of apoptosis, function as markers of genomic imprinting, and act as competing endogenous RNAs (ceRNAs) that share micro RNAs (miRNA) biding sites [(3-5)] Dysregulation of lncRNA expression among various cancers has been implicated to have a potential effect on tumorigenesis [(6, 7)] Increasing number of lncRNAs have been characterized in different malignancies and they are mainly involved in the modulation of carcinogenesis and cancer progression [(8)].

Papillary thyroid carcinoma susceptibility candidate 3 (PTCSC3) is an intergenic long noncoding RNA. It was reported to be involved in tumor suppression in thyroid carcinoma[(9)]. The PTCSC3 gene is exclusively significantly suppressed in PTC tumor tissues [(10)]. Studies have shown that lncRNA PTCSC3 downregulates the expression of S100A4 gene, leading to reduced cell motility and invasiveness[(11)]. S100A4 is a Ca^{2+}-binding protein that are associated with diverse cellular processes, there aer cell invasion, proliferation and cell-cell interaction [(12-14)]. S100A4 was reported to be overexpressed in human PTC tissues and lymph node metastases [(15, 16)], and knockdown of S100A4 inhibited the growth and

metastasis in anaplastic papillary thyroid carcinomas cells [17]. VEGF and MMP-9 are downstream targets of S100A4 and the suppression of S100A4 also results in suppressed expressions about VEGF and MMP-9, which in turn suppresses the invasion of thyroid carcinoma cells [18, 19] VEGF is an essential endothelial cell mitogen and is an important factor in angiogenesis [20]. Studies have shown that increased expression of VEGF promotes thyroid carcinoma cell growth and migration, while the decreased expression of VEGF inhibits tumor growth [21]. MMP-9 has also been shown to associated with the migration and survival of endothelial cells [22, 23], Caspase-3 and Caspase-9 are two essential caspases that play critical roles in apoptosis, which is the process of programmed cell death [24, 25].

Thus, it is significant to research the effects and potential mechanisms of the lncRNA PTCSC3 on the angiogenesis and growth of thyroid carcinoma xenografts, which might provide a direction for treating papillary thyroid carcinomas.

2. Materials And Methods

2.1 Cell culture

The thyroid cell line Nthy-ori 3-1 (JN-2993, Shanghai Ji Ning Industrial Co., Ltd., China), and several human thyroid carcinoma cell lines including SW579 (HTB-107, ATCC, USA), TPC-1 (CC-Y1522, Shanghai Enzyme Research Biotechnology Co., Ltd., China), BCPAP (HTX-1878, Shenzhen Haodi Huatuo Biotechnology Co., Ltd., China) and K1 (HTX-2011, Shenzhen Haodi Huatuo Biotechnology Co., Ltd., China) were obtained. The cells were maintained in RPMI 1640 medium (Gibco, Thermofisher, NY, USA) with 10% fetal bovine serum (Sigma-Aldrich, St. Louis, MO, USA), and cultured at 37 °C in 5% CO_2 .

2.2 RT-PCR

Total RNAs were extracted through Trizol (15596018, Invitrogen, Carlsbad, CA, USA). RNAs were then reversely transcribed into cDNA by reverse transcription kit (Applied Biosystems, Waltham, MA, USA). The Mastercycler® nexus X2 (Eppendorf, Hamburg, Germany) was used for qRT-PCR following the manufacture's protocol. The cycling conditions for PTCSC3 and S100A4 are as follows: 95 °C for 5 min, 40 cycles of 95 °C for 30 s, 60 °C for 60 s. Using GAPDH as an internal reference. Relative expressions were calculated via the $2^{-\Delta\Delta Ct}$ method. The sequences of primers are listed as follows:.

PTCSC3 Forward: 5'- TCAAACTCCAGGGCTTGAAC -3'

Reverse: 5'- ATTACGGCTGGGTCTACCT -3'

S100A4 Forward: 5'- TCAGAACTAAAGGAGCTGCTGACC-3'

Reverse: 5'- TTTCTTCCTGGGCTGCTTATCTGG -3'

GAPDH Forward: 5'- AGCCCATCACCATCTTCCAG -3'

Reverse: 5'- CCTGCTTCACCACCTTCTTG -3'

2.3 Cell transfection for PTCSC3 and grouping

Thyroid carcinoma cells with the highest differential expression of PTCSC3 were selected for transfections. The cells were digested with trypsin (Invitrogen, Carlsbad, CA, USA) and 2×10^5 cells in logarithmic phase of growth were used for seeding into six-well plates. After 24 h, the cell growth was observed under inverted microscope until the cell density reached 80-90%. The cells were divided into five group: control group (no treatment), PTCSC3 overexpression negative control group (NC1), PTCSC3 overexpression group (PTCSC3), PTCSC3 inhibitor negative control group (NC1) and PTCSC3 inhibitor group (si-P). The lentivirus plasmids were constructed by Shanghai Genechem Co., Ltd. The transfection efficiency was tested by RT-PCR after 24h.

2.4 CCK8

Logarithmic cells were seeded into 96-well plates with 2×10^4/ml with 100 μl of medium added to each well. After culture for 24h, 48h, 72h and 96h at 37 ℃ and 5% CO_2. Then 10 μl CCK-8 solution was added to each well (tonghua institute of chemistry, Japan) and mixed well for further culture for 4h. The absorbance (OD) of each well at 450 nm was measured by the microplate reader.

2.5 Clone formation assay

The density was modulated to 250 cells/ml, and 2ml cells were added to each well of the six-well plate. The cells were incubated at 37℃ and 5%CO2 for 2-3 weeks, then fresh medium was changed every three days. The cells were fixed with methanol, 1ml gemsa solution was added to each well, and the cells were stained for 30min. The cells were washed with ultrapure water for 2 times, and the water around the dish was sucked off with a filter. Take pictures with a camera.

2.6 Transwell assay

Invasion: pre-cooled RPMI1640 medium was mixed with Matrigel (solebau, Beijing) at 1:1, and evenly spread at the bottom of the upper chamber of Transwell at 50μl per well (Corning Life Sciences, Corning, NY). And 100 μl lung cancer cell suspension (5×10^4) were added to each well and incubated at 37℃ for 4h. In the lower chamber, 600 μl RPMI1640 medium was added and incubated at 37℃ and 5% CO_2 for 72h. The chamber was removed, washed twice with PBS, and fixed at 4℃ with 5% glutaraldehyde. It was washed with PBS twice, added 0.1% crystal violet (Beijing solabao) for 30min, washed with PBS twice. Five fields (400×) were randomly selected under an inverted microscope (Olympus, Japan) to calculate the mean value. Migration: no Matrigel was used in Transwell chamber. Other steps were the same as invasion.

2.7 Tube formation assay

Firstly, 50 μL Matrigel (BD Bioscience, USA) was applied to 96-well plates and cured at 37℃ for 1h. Then, HUVECs were digested and centrifuged at 1000rpm for 5min. The cell supernatants (4×104 cells/wells) were resuspended and inoculated on the matrix glue, placed in the medium, and incubated at 37℃ in an incubator with 5% CO2 (Thermo, USA) for 48h. The digital images were obtained by counting under an inverted microscope using the digital Camera system on the microscope (Jenoptik ProgRes Camera, Germany).

2.8 Flow cytometry

After treatment, the cells were cultured for 24 hours then collected. The cells were resuscitated by precooling with 1×PBS (4℃), centrifuged at 1000rpm for 5-10 minutes, and washed. Then 300 μl of 1×Binding Buffer was added to suspend the cells. Annexin V-APC of 5 μl was added and mixed, then incubated for 15 minutes at room temperature without light. Five minutes before loading, 5 μl of PI was added for dyeing, and 200 μl of 1×Binding Buffer was added before loading. The samples were finally detected by flow cytometry (Beckman Coulter, Brea, CA, USA) and analyzed by CellQuest software (BD Bioscience, San Diego, CA).

2.9 Western blot

After cell lysis, the supernatant was taken after centrifugation (2000rpm, 20min). The BCA kit (Solarbio, Beijing, China) was used to measure the protein concentration. And 40 L of protein samples were mixed with 10% SDS gel buffer at 1:1 then heated at 95℃ for 5min to denature the protein. PVDF membrane (Merck, Darmstadt, Germany) was transferred at a voltage of 80V for 30min and sealed with TBST solution containing 5% skim milk powder at 4℃ for 1h. Rabbit anti-human Bax (1:500, orb224426, Biorbyt, Cambridge, UK) and Bcl-2 (1:500, orb226346, Biorbyt, Cambridge, UK), Cleaved caspase-3 (1:500, orb126597, Biorbyt, Cambridge, UK), S100A4 (1:500, orb254558, Biorbyt, Cambridge, UK), β-actin (1:2000, orb178392, Biorbyt, Cambridge, UK) polyclonal antibodies were diluted with TBST solution containing 3% bovine serum protein at 4℃ overnight. After rewarming, horseradish peroxidase-labeled goat anti-rabbit IgG (1:1000, ABIN101988, linates-online, Aachen, Germany) were incubated for 1h, washed and colored with ECL luminescent substrate for 3-5min. Protein expression level was standardized by β-actin. And gray level was scanned and quantified by Image J (NIH) software.

In the nude mice experiment, the primary antibodies were rabbit anti-human VEGF (1:500, orb27288, Biorbyt, Cambridge, UK) and MMP-9-9 (1:500, orb227878, Biorbyt, Cambridge, UK) polyclonal antibodies. The other steps are the same as above.

2.10 Cell transfection for PTCSC3 and S100A4, and grouping

(1) Control group; (2) PTCSC3 overexpression group (PTCSC3); (3) S100A4 silence negative control group (NC3); (4) S100A4 silence group (si-S); (5) PTCSC3 overexpression+S100A4 overexpression negative control group (P+NC4); (6) PTCSC3 overexpression+S100A4 overexpression group (P+S). The transfection efficiency of S100A4 was determined by qRT-PCR, and the above experiments were repeated.

2.11 Construction and grouping of nude mice with xenograft tumors

Twenty-four SPF Balb/c female nude mice, 16-18g, 4 weeks old, purchased from Charles River. License number SCXK (Beijing) was 20160006. The nude mice were fed in the aseptic, independent and air supply isolation cage at air laminar flow purification room, where kept the constant temperature (26-28℃) and humidity (relative humidity 40%-60%). Feed, drinking water and bedding material were sterilized. Animal experiments followed the guidelines of NIH (NIH pub.no.85-23, revised 1996), which have been approved by the animal protection and use committee of the 960^{th} Hospital of the PLA Joint Logistics Support Force. Cells in the logarithmic growth phase were digested with 0.25% trypsin. Cells were collected and counted. The concentration was adjusted to 2.5×10^{6} /ml. And 0.2 ml was inoculated on the right forelimb close to soft skin on the back of the nude mice. Twenty-four nude mice were randomly divided into (1) Control group. (2) PTCSC3 overexpression group (PTCSC3); (3) S100A4 silence group (si-s); (4) PTCSC3 overexpression + S100A4 overexpression group (P+S), 6 in each group.

2.12 Tumor volume calculation

Vernier calipers were used to measure tumor length (L) and short diameter (W) every 7 days to calculate tumor volume. Tumor volume (V) = (long diameter × short diameter 2) /2. After 35 days, the nude mice were anesthetized by intraperitoneal injection of 0.6% pentobarbital sodium (40mg/kg). The mice were sacrificed by neck dissection. The tumor tissue was collected and weighed. The tumor tissue was fixed in 4% paraformaldehyde and embedded in paraffin for 24 hours. Part of the tissues was placed in the freezer tube and stored in the refrigerator at -80℃.

2.13 Immunochemistry

After routine sections of the tumor tissue, the toasted slides were dewaxed with xylene and hydrated with gradient ethanol solution. And 3% H2O2 methanol solution was used to inactivat for 20min, followed by high-temperature antigen thermal repair in citrate buffer (pH6.0) for 10min and 5%BSA for 20min. Rabbit anti-human Ki67 (1:200, orb88614, Biorbyt, Cambridge, UK) polyclonal antibodies were added and reacted overnight at 4℃. After rewarming, horseradish peroxidase-labeled goat anti-rabbit IgG (1:1000, ABIN101988, linats-online, Germany) were incubated with secondary antibodies. The sections were stained, redyed, dehydrated, transparent and sealed. After observation under a ×400 optical microscope (Olympus, Japan), AperioImagescope11.1 software was used to count, and the result was expressed as the percentage (%) of positive cells. Microvascular density (MVD) was calculated by immunohistochemistry of CD31 (1:200, orb88916, Biorbyt, Cambridge, UK) in tumor blood vessels. MVD was calculated by reference to Weidner count. High-vascular density area (hot-spot) was selected at 100× field. MVD of 5 fields was counted at 400× field. The mean value was taken as the MVD value of the tumor.

2.14 TUNEL

The thickness of the section was 4 μm. After conventional dewaxing of xybenzene and dehydrating with gradient ethanol, apoptosis detection kit (No.: ZK-8005, ZSGB-BIO, China) was used for quantitative detection of apoptosis by TUNEL. Five fields were randomly selected under a 400-x optical microscope (BX50 /Olympus, Japan). Cell lines were identified as apoptotic cells with brown or tan granules and apoptotic cell morphological characteristics. Apoptotic index (AI) was calculated to reflect the degree of apoptosis. Apoptotic index = (number of apoptotic positive cells /total number of cells) ×100%

2.15 Statistical analysis

SPSS 19.0 was used for data processing. Data analysis results were presented as mean±SD. T test was used for data analysis between two groups. ANOVA was used for data analysis between multiple groups. And Dunnett-t test was used for subsequent analysis. The relationship between the expression difference in PTCSC3 and S100A4 and the clinicopathological characteristics of papillary thyroid carcinomas patients was analyzed by chi-square test. The correlation between PTCSC3 and S100A4 expression was analyzed by Pearson correlation analysis. P <0.05 indicated that the difference was statistically significant.

3. Results

3.1 The effect of PTCSC3 on the proliferation of human papillary thyroid carcinomas cells

As shown in Figure 1, compared with Nthy-ori 3-1, the expression of PTCSC3 mRNA in human papillary thyroid carcinomas cells was obviously decreased ($p<0.05$), while the expression of S100A4 mRNA was visibly increased ($p<0.05$). The differential expression was most pronounced in TPC-1 cells. TPC-1 cells were selected for subsequent experiments. Compared to the control group, there was no obvious difference in PTCSC3 mRNA expression, cell proliferation, invasion, migration and tube formation ability between the NC1 and NC2 groups ($p>0.05$). The level of PTCSC3 mRNA was obviously increased in PTCSC3 group, and the cell proliferation, invasion, migration and tube formation ability were significantly decreased ($p<0.05$). The expression of PTCSC3 mRNA was visibly decreased in the si-P group, and cell proliferation, invasion, migration and tube formation capacity were significantly increased ($p<0.05$).In comparation with the PTCSC3 group, the expression of PTCSC3 mRNA was significantly decreased in the si-P group, and the cell proliferation, invasion, migration and tube formation ability were significantly increased ($p<0.05$).

3.2 The effect about PTCSC3 on apoptosis of human papillary thyroid carcinomas cells

As shown in Figure 2, in comparation with the control group, the apoptosis rate and the expression of apoptosis-related protein Bax, Cleaved caspase-3 of the PTCSC3 group was visibly increased, while the level of Bcl-2 protein was decreased. However, the results of si-P group were opposite ($p<0.05$). Compared to PTCSC3 group, the apoptosis rate and the expression of apoptosis-related protein of si-P group were significantly decreased, while Bcl- 2 protein level was markedly increased ($p < 0.05$).

3.3 PTCSC3 regulates the effect of S100A4 on the proliferation of human papillary thyroid carcinomas cells

As shown in Figure 3, the expression of S100A4 gene and protein was significantly decreased in the PTCSC3 group compared with the Control group, whereas that in the si-P group was increased ($p<0.05$). Compared to the PTCSC3 group, the expression of S100A4 gene and protein in the si-P group was markedly increased ($p<0.05$). Compared to the control group, the expression of S100A4 mRNA was significantly decreased in the PTCSC3, si-S, P+NC4, and P+S groups ($p<0.05$). In comparation with the PTCSC3 and si-S groups, the expression of S100A4 mRNA was obviously increased in the P+S group ($p<0.05$). Compared to the control group, the proliferation, invasion, migration, and tube formation ability of the PTCSC3, si-S, P+NC4, and P+S groups were visibly lower ($p<0.05$). Compared with the PTCSC3 and si-S groups, the proliferation, invasion, migration and tube formation ability of P+S group were significantly increased ($p<0.05$).

3.4 PTCSC3 regulates the effect of S100A4 on apoptosis of human papillary thyroid carcinomas cells

In Figure 4, in comparation to control group, the apoptosis rate and the expression of apoptosis-related protein of PTCSC3, si-S, P+NC4 and P+S groups were effectively promoted, while the level of Bcl-2 was obviously inhibited ($p<0.05$). Compared to PTCSC3 and si-S group, the apoptosis rate and the expressions of Bax and Cleaved caspase-3 of P+S group were significantly down regulated. The Bcl-2 protein expression was significantly promoted ($p<0.05$).

3.5 PTCSC3 regulates the effect of S100A4 on tumor growth

In Figure 5, compared to the control group, the tumor growth rate, volume and weight of the other groups were reduced, while the percentage of Ki67 positive cells, MVD values and expressions of VEGF and MMP-9 in the tumor tissues were obviously down-regulated($p<0.05$). Compared to PTCSC3 and si-S group, the tumor growth rate of P+S group was significantly accelerated, the tumor volume and weight were visibly increased, while the percentage of Ki67 positive cells, MVD values, and protein expressions of VEGF and MMP-9 in tumor tissues were effectively increased ($p<0.05$).

3.6 PTCSC3 regulates the effect of S100A4 on tumor apoptosis

In the figure 6, compared to control group, the apoptotic index and the expressions of apoptosis-related protein in other groups were significantly increased. But expression of Bcl-2 was visibly prohibited ($p<0.05$). Compared to PTCSC3 and si-S group, the tumor apoptotic index and the expressions of Bax and Cleaved caspase-3 in P+S group was significantly down-regulated, and the expression of Bcl-2 protein was significantly promoted ($p<0.05$).

4. Discussions

LncRNA PTCSC3 has been shown to affect the development of papillary thyroid carcinoma [11]. To elucidate the biological functions of PTCSC3, thyroid carcinoma xenografts models in nude mice were constructed with gain-of-function experiments in thyroid carcinoma cell lines. The results indicated that overexpression of PTCSC3 inhibited the formation of thyroid carcinoma xenograft tumor and angiogenesis. The roles of dysregulated lncRNAs in carcinogenesis and cancer progression have been widely investigated in various studies [8]. Different lncRNAs have been continuously identified in different types of malignancies. For instance, increased expression of LncRNA H19 and resulting cell proliferation in pancreatic ductal adenocarcinoma [26]. LncRNA HULC was first found to be highly expressed in liver cancer and was identified as an oncogene in glioma [27]. LncRNA BISPR regulates the microRNA miR-21-5p and promotes the progression of thyroid papillary carcinoma [28]. The studies suggested that the signaling network of lncRNAs regulated cancer development is complex and needs thorough investigations.

To elucidate the potential mechanisms by which PTCSC3 regulates the thyroid carcinoma cell invasion, the functions of S100A4 with gain-of-function experiments were also investigated. The data also illustrated that the abundant expression of PTCSC3 in the TPC-1 cell lines correlated with significantly suppressed expression of S100A4. Downstream target genes of S100A4 were also investigated in this study in order to elucidate how S100A4 functions in promoting thyroid carcinomas cell invasion and proliferation. VEGF and MMP-9 are two major genes that been characterized as downstream of S100A4 and depletion of S100A4 in thyroid carcinoma cells restrain their capabilities of proliferation, angiogenesis and invasion by down regulating the expression of VEGF and MMP-9. In this study, we detected the level of VEGF and MMP-9 and showed that they were significantly up regulated with abundant presence of S100A4, which confirmed that the underlying mechanism of PTCSC3 down regulates the expression of S100A4. Eventually, it leads to reduced expression of VEGF and MMP-9 and ultimately the suppression of thyroid carcinomas tumor development. The VEGF signaling pathway can affect EMT and tumor differentiation [29, 30]. MMPs also have been shown to promote invasion of blood vessels and lymphatics by digesting extracellular substrates in the development of cancers [31]. Some have reported that MMPs facilitate the induction of the EMT pathway [32]. These emerging correlations also lead to us to reveal possible relationships between leading actors in the EMT developed in thyroid carcinomas cells.

Genes involved in the apoptosis caspase pathways were also investigated in this study to further understand the mechanisms of regulations between PTCSC3 and S100A4 in suppression of thyroid carcinomas tumor development. Studies have reported distinct roles of caspase family members during intrinsic apoptosis. Caspases involved in apoptosis have been classified by their actions into initiator caspases (Caspase-8 and -9) and inhibitor caspases (Caspase-3, -6 and -7) [33]. In the present study, the expression of Caspase-3 was detected and the results showed that they were significantly suppressed with abundant presence of S100A4. The results demonstrated that the potential mechanism of PTCSC3 down regulates the expression of S100A4, which in turn leads to abundance of Caspase-3 and ultimately promoting apoptosis of thyroid carcinomas tumor cells. Previous studies also reported other targeted

gene for PTCSC3, for example the tumor suppressor gene neuregulin-1 (NRG1) involved in interactions with PTCSC3 in thyroid carcinoma [34, 35]. A recent study of glioma revealed that PTCSC3 inhibits the proliferation and invasion of glioma cells and suppressed the epithelial-mesenchymal transition (EMT) by regulating the Wnt/β-catenin signaling pathway [36]. Therefore, besides the regulation through S100A4, the possible mechanisms that PTCSC3 regulates the proliferation and invasion of cancer cells could be complicated and involve multiple signaling pathways. Therefore, more investigations such as genome wide association studies are needed to reveal potential pathways involved in the regulations of PTCSC3 or S100A4.

5. Conclusion

In conclusion, the overexpression of PTCSC3 inhibits proliferation, invasion, metastasis and angiogenesis of thyroid carcinomas cells, and also promotes apoptosis of thyroid carcinomas cells *in vivo*. These functions of PTCSC3 are regulated by the suppression of S100A4 pathway through downstream targeting genes. Regulation of LncRNA PTCSC3 and S100A4 could be an effective potential therapeutic and preventive approach for thyroid carcinomas.

Declarations

Ethics approval and consent to participate

Animal experiments were followed the NIH guidelines (NIH Pub. No. 85-23, revised 1996) and have been approved by the Animal Protection and Use Committee of Huai'an Second People's Hospoital.

Consent for publication

Not applicable

Availability of data and materials

The datasets used and/or analysed during the current study are available from the corresponding author on reasonable request.

Competing interests

The authors declare that they have no competing interests.

Funding

Not applicable.

Authors' contributions

Q W and L Jcarried out the experimental work and the data collection and interpretation. Q W and Y Z participated in the design and coordination of experimental work, and acquisition of data. L Jnd J W participated in the study design, data collection, analysis of data and preparation of the manuscript. Q W and H D carried out the study design, the analysis and interpretation of data and drafted the manuscript. All authors read and approved the final manuscript.

Acknowledgements

Not applicable.

References

1. Eheman C, Henley SJ, Rachel B-B, Eric JJ, Maria JS, Anne-Michelle N, Liping P, Robert NA, Janet EF, Betsy AK. 2012. Annual Report to the Nation on the status of cancer, 1975-2008, featuring cancers associated with excess weight and lack of sufficient physical activity. Cancer 118:2338-2366.
2. Jemal A, Ms. Rebecca S, Dr. Elizabeth W, Mr. Taylor M, Mr. Jiaquan X, Dr. Michael JT. 2007. Cancer Statistics, 2007. CA A Cancer Journal for Clinicians 57:43-66.
3. Struhl, Kevin. 2007. Transcriptional noise and the fidelity of initiation by RNA polymerase II. Nature Structural & Molecular Biology 14:103-105.
4. Gupta RA, Shah N, Wang KC, Kim J, Horlings HM, Wong DJ, Tsai M-C, Hung T, Argani P, Rinn JL. 2010. Long non-coding RNA HOTAIR reprograms chromatin state to promote cancer metastasis. Nature 464:1071-1076.
5. Salmena L, Laura P, Yvonne T, Lev K, Pier?Paolo P. 2011. A ceRNA Hypothesis: The Rosetta Stone of a Hidden RNA Language? Cell 146:353-358.
6. Qi P, Du X. 2013. The long non-coding RNAs, a new cancer diagnostic and therapeutic gold mine. Modern Pathology 26:155-165.
7. Kogo R, Shimamura T, Mimori K, Kawahara K, Imoto S, Sudo T, Tanaka F, Shibata K, Suzuki A, Komune S. 2011. Long Noncoding RNA HOTAIR Regulates Polycomb-Dependent Chromatin Modification and Is Associated with Poor Prognosis in Colorectal Cancers. Cancer Research 71:6320-6326.
8. Huarte M. 2015. The emerging role of lncRNAs in cancer. Nature Medicine 21:1253-1261.
9. Fan M, Li X, Jiang W, Huang Y, Li J, Wang Z. 2013. A long non-coding RNA, PTCSC3, as a tumor suppressor and a target of miRNAs in thyroid cancer cells. Experimental & Therapeutic Medicine 5:1143—1146.
10. Jendrzejewski J, He H, Radomska HS, Li W, Tomsic J, Liyanarachchi S, Davuluri RV, Nagy R, de la Chapelle A. 2012. The polymorphism rs944289 predisposes to papillary thyroid carcinoma through a large intergenic noncoding RNA gene of tumor suppressor type. Proceedings of the National Academy of Sciences of the United States of America 109:8646-8651.

11. Jendrzejewski J, Thomas A, Liyanarachchi S, Eiterman A, Albert de la C. 2015. PTCSC3 Is Involved in Papillary Thyroid Carcinoma Development by Modulating S100A4 Gene Expression. J Clin Endocrinol Metab 100:1370-1377.
12. Mohammad S, Mee-Hyang K, Jeremy James J, Vaqar Mustafa A, Irina E, Naghma K, Bilal BH, Bhat KMR, Sami S, Shannon RS. 2006. S100A4 accelerates tumorigenesis and invasion of human prostate cancer through the transcriptional regulation of matrix metalloproteinase 9. Proceedings of the National Academy of Sciences of the United States of America 103:14825-14830.
13. Ismail TM, Zhang S, Fernig DG, Gross S, Martin-Fernandez ML, See V, Tozawa K, Tynan CJ, Wang G, Wilkinson MC. 2010. Self-association of Calcium-binding Protein S100A4 and Metastasis. Journal of Biological Chemistry 285:914-922.
14. Sun X, Wang Y, Zhang J, Tu J, Wang XJ, Su XD, Wang L, Zhang Y. 2012. Tunneling-nanotube direction determination in neurons and astrocytes. Cell Death & Disease 3:e438.
15. Hyman DM, Puzanov I, Subbiah V, Faris JE, Chau I, Blay J-Y, Wolf J, Raje NS, Diamond EL, Hollebecque A. 2015. Vemurafenib in Multiple Nonmelanoma Cancers with BRAF V600 Mutations. New England Journal of Medicine 373:726-736.
16. Min HS, Choe G, Kim S-W, Park YJ, Park DJ, Youn Y-K, Park SH, Cho BY, Park SY. 2008. S100A4 expression is associated with lymph node metastasis in papillary microcarcinoma of the thyroid. Mod Pathol 21:748-755.
17. Zhang K, Yu M, Hao F, Dong A, Chen D. 2016. Knockdown of S100A4 blocks growth and metastasis of anaplastic thyroid cancer cells in vitro and in vivo. Cancer Biomarkers 17:281-291.
18. Jia W, Gao XJ, Zhang ZD, Yang ZX, Zhang G. 2013. S100A4 silencing suppresses proliferation, angiogenesis and invasion of thyroid cancer cells through downregulation of MMP-9 and VEGF. European Review for Medical & Pharmacological Sciences 17:1495-1508.
19. Donato R, Cannon BR, Sorci G, Riuzzi F, Hsu K, Weber DJ, Geczy CL. 2013. Functions of S100 proteins. Current molecular medicine 13:24-57.
20. Carmeliet P, Jain RK. 2000. Angiogenesis in cancer and other disease. Nature 407.
21. Lin JD, Chao TC. 2005. Vascular endothelial growth factor in thyroid cancers. Cancer Biother Radiopharm 20:648-661.
22. Kitajima K, Koike J, Nozawa S, Yoshiike M, Takagi M, Chikaraishi T. 2011. Irreversible immunoexpression of matrix metalloproteinase-9 in proximal tubular epithelium of renal allografts with acute rejection. Clinical Transplantation 25:336-344.
23. Rundhaug JE. 2005. Matrix metalloproteinases and angiogenesis. Journal of Cellular and Molecular Medicine 9:267-285.
24. Porter AG, J?nicke RU. 1999. Emerging roles of caspase-3 in apoptosis. Cell Death & Differentiation 6:99-104.
25. Hua Z, Li Y, Liu X, Wang X. 1999. An APAF-1·Cytochrome c Multimeric Complex Is a Functional Apoptosome That Activates Procaspase-9 *. Journal of Biological Chemistry 274:11549-11556.

26. Ma L, Tian X, Wang F, Zhang Z, Yang Y. 2016. The long noncoding RNA H19 promotes cell proliferation via E2F-1 in pancreatic ductal adenocarcinoma. Cancer Biology & Therapy 17:1051-1061.
27. Zhu Y, Zhang X, Qi L, Cai Y, Yang P, Xuan G, Jiang Y. 2016. HULC long noncoding RNA silencing suppresses angiogenesis by regulating ESM-1 via the PI3K/Akt/mTOR signaling pathway in human gliomas. Oncotarget 7:14429-14440.
28. Hong Z, Cai Y, Zheng L, Zhang Z, Lin X, Jiang N. 2018. LncRNA BISPR promotes the progression of thyroid papillary carcinoma by regulating miR-21-5p. International Journal of Immunopathology & Pharmacology 32:2058738418772652.
29. Goel HL, Mercurio AM. 2013. VEGF targets the tumour cell. Nature Reviews Cancer 13:871-882.
30. Mak P, Leav I, Pursell B, Bae D, Yang X, Taglienti CA, Gouvin LM, Sharma VM, Mercurio AM. 2010. ERbeta Impedes Prostate Cancer EMT by Destabilizing HIF-1α and Inhibiting VEGF-Mediated Snail Nuclear Localization: Implications for Gleason Grading. Cancer Cell 17:319-332.
31. Wolf K, Friedl P. 2011. Extracellular matrix determinants of proteolytic and non-proteolytic cell migration. Trends in Cell Biology 21:736-744.
32. Kalluri R, Weinberg RA. 2009. The basics of epithelial-mesenchymal transition. Journal of Clinical Investigation 119:1420-1428.
33. McIlwain DR, Berger T, Mak TW. 2013. Caspase Functions in Cell Death and Disease. Cold Spring Harbor Perspectives in Biology 5:a008656-a008656.
34. Rogounovitch TI, Bychkov A, Takahashi M, Mitsutake N, Nakashima M, Nikitski AV, Hayashi T, Hirokawa M, Ishigaki K, Shigematsu K, Bogdanova T, Matsuse M, Nishihara E, Minami S, Yamanouchi K, Ito M, Kawaguchi T, Kondo H, Takamura N, Ito Y, Miyauchi A, Matsuda F, Yamashita S, Saenko VA. 2015. The Common Genetic Variant rs944289 on Chromosome 14q13.3 Associates with Risk of Both Malignant and Benign Thyroid Tumors in the Japanese Population. Thyroid 25:333-340.
35. Gudmundsson J, Sulem P, Gudbjartsson DF, Jonasson JG, Masson G, He H, Jonasdottir A, Sigurdsson A, Stacey SN, Johannsdottir H, Th Helgadottir H, Li W, Nagy R, Ringel MD, Kloos RT, de Visser MCH, Plantinga TS, den Heijer M, Aguillo E, Panadero A, Prats E, Garcia-Castaño A, De Juan A, Rivera F, Walters GB, Bjarnason H, Tryggvadottir L, Eyjolfsson GI, Bjornsdottir US, Holm H, Olafsson I, Kristjansson K, Kristvinsson H, T Magnusson O, Thorleifsson G, Gulcher JR, Kong A, Kiemeney LALM, Jonsson T, Hjartarson H, Mayordomo JI, Netea-Maier RT, de la Chapelle A, Hrafnkelsson J, Thorsteinsdottir U, Rafnar T, Stefansson K. 2012. Discovery of common variants associated with low TSH levels and thyroid cancer risk. Nature Genetics 44:319-322.
36. Xia S, Ji R, Zhan W. 2017. Long noncoding RNA papillary thyroid carcinoma susceptibility candidate 3 (PTCSC3) inhibits proliferation and invasion of glioma cells by suppressing the Wnt/β-catenin signaling pathway. BMC Neurology 17:30.

Figures

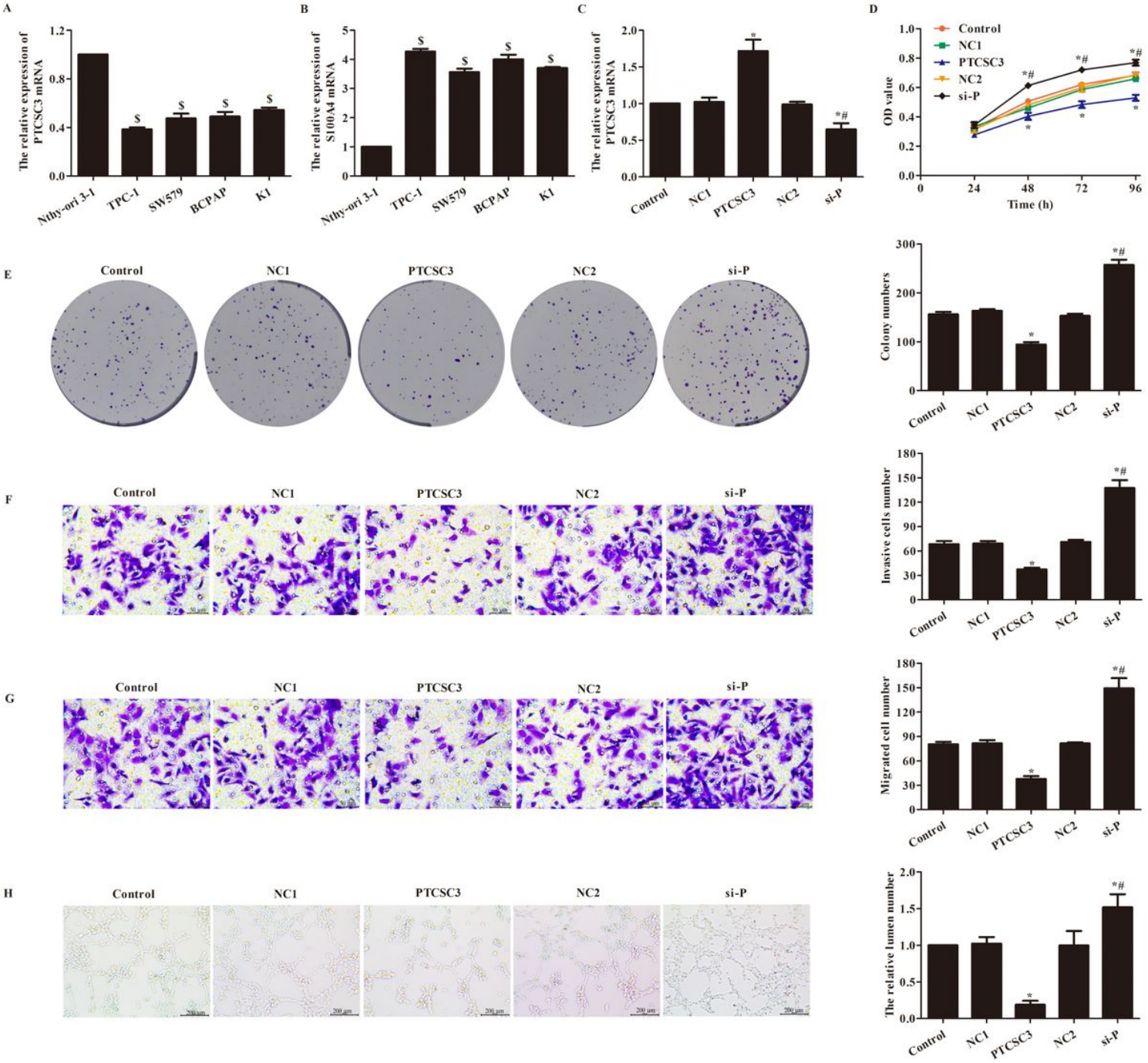

Figure 1

Effect about PTCSC3 on proliferation of human papillary thyroid carcinomas cells. (A) RT-PCR of PTCSC3 expression in cells; (B) RT-PCR of S100A4 expression in cells; (C) RT-PCR of PTCSC3 expression in transfected cells; (D) CCK8 detection Cell proliferation ability; (E) colony assay to detect cell proliferation; (F) Transwell assay for cell invasion (x400); (G) Transwell assay for cell migration (x400); (H) tube formation The experiment was conducted to observe the ability of tube formation in vitro (×200). Compared with the Nthy-ori 3-1 group, $p<0.05; and compared to the control group, *p<0.05; compared to PTCSC3, # p<0.05. Data analysis results were repeated 3 times and presented as mean±SD. ANOVA was used for data analysis between multiple groups. And Dunnett-t test was used for subsequent analysis.

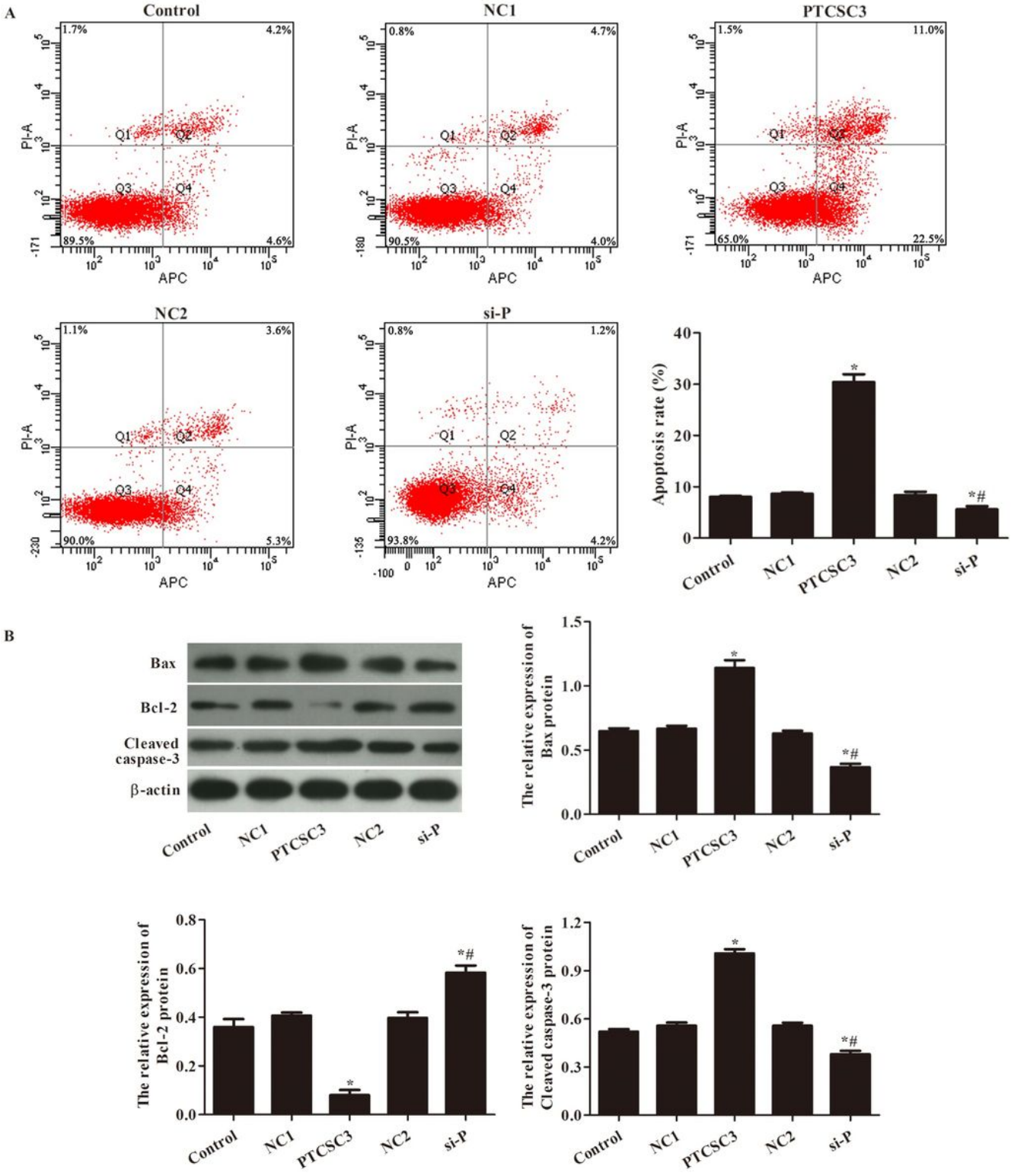

Figure 2

Effect of PTCSC3 on apoptosis in human papillary thyroid carcinomas cells. (A) Apoptosis; (B) Western blot. compared to the control group , *p<0.05; compared to PTCSC3 group, #p<0.05. Data analysis results were repeated 3 times and presented as mean±SD. ANOVA was used for data analysis between multiple groups. And Dunnett-t test was used for subsequent analysis.

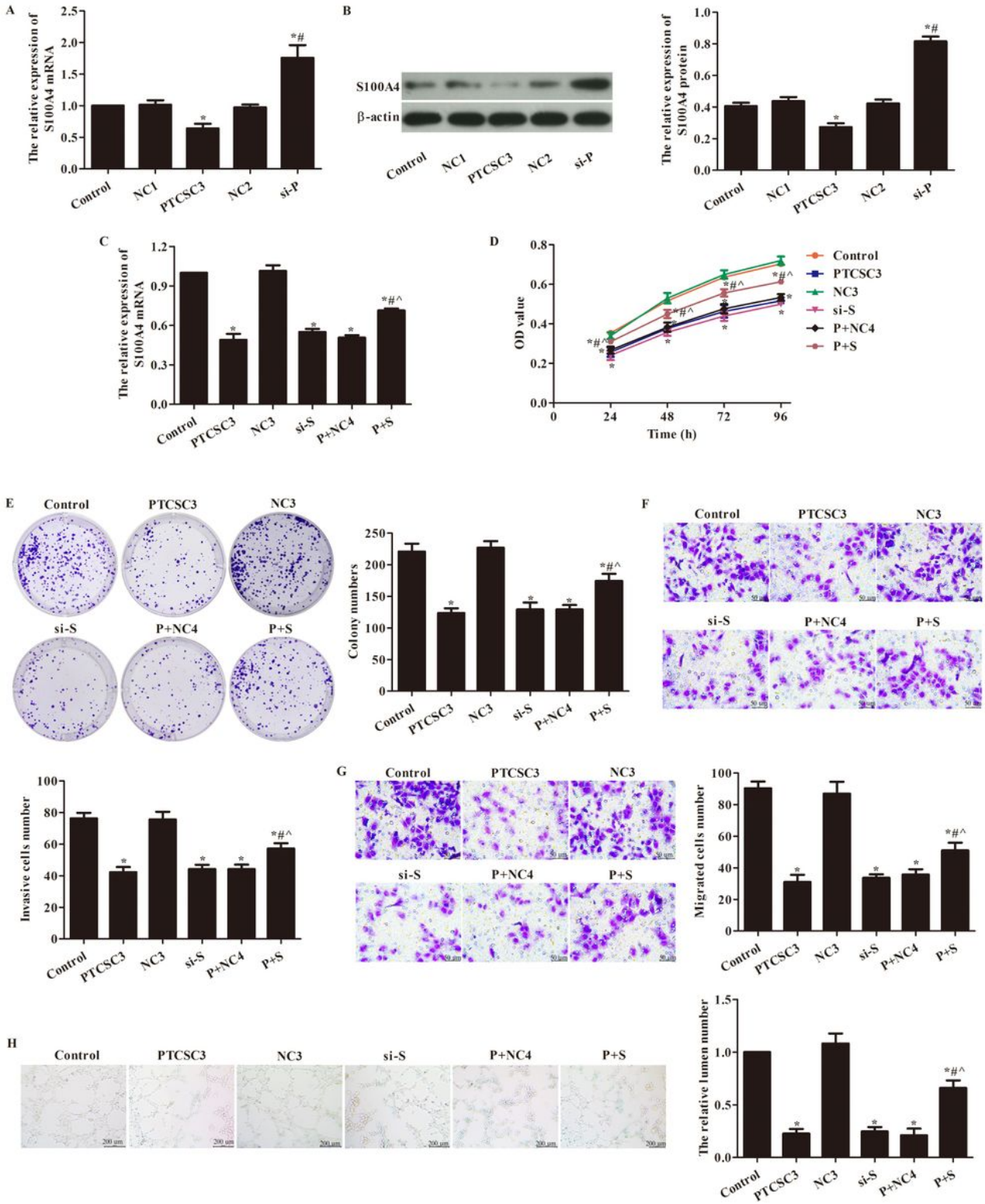

Figure 3

PTCSC3 regulates the roles of S100A4 about proliferation of human papillary thyroid carcinomas cells. (A) RT-PCR of S100A4 expression in cells; (B) WB analysis of S100A4 protein expression; (C) RT-PCR of S100A4 expression in transfected cells; (D) CCK8 detection cells Proliferative capacity; (E) Clonal formation assay to detect cell proliferation; (F) Transwell assay for cell invasion (×400); (G) Transwell assay for cell migration (×400); (H) Tube formation assay The in vitro tube formation ability (x100) was

observed. Compared to the control group, *p<0.05; compared to PTCSC3, #p<0.05; compared to si-S group, ^ p<0.05. Data analysis results were repeated 3 times and presented as mean±SD. ANOVA was used for data analysis between multiple groups. And Dunnett-t test was used for subsequent analysis.

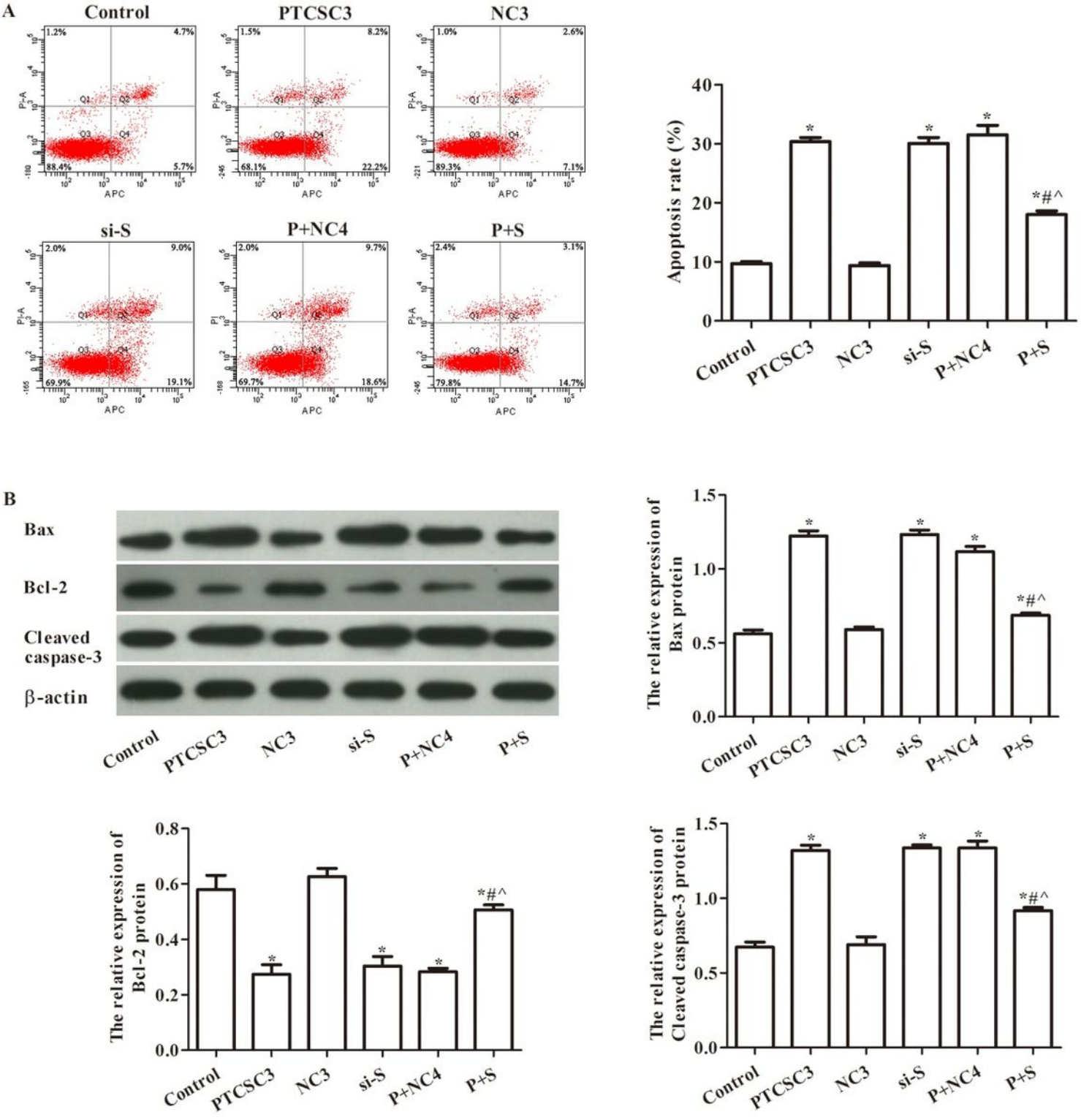

Figure 4

PTCSC3 regulates the effects of S100A4 on apoptosis in human papillary thyroid carcinomas cells. (A) Apoptosis; (B) Western blot. Compared to the control group, *p<0.05; compared to PTCSC3, #p<0.05;

compared to si-S group, ^ p<0.05. Data analysis results were repeated 3 times and presented as mean±SD. ANOVA was used for data analysis between multiple groups. And Dunnett-t test was used for subsequent analysis.

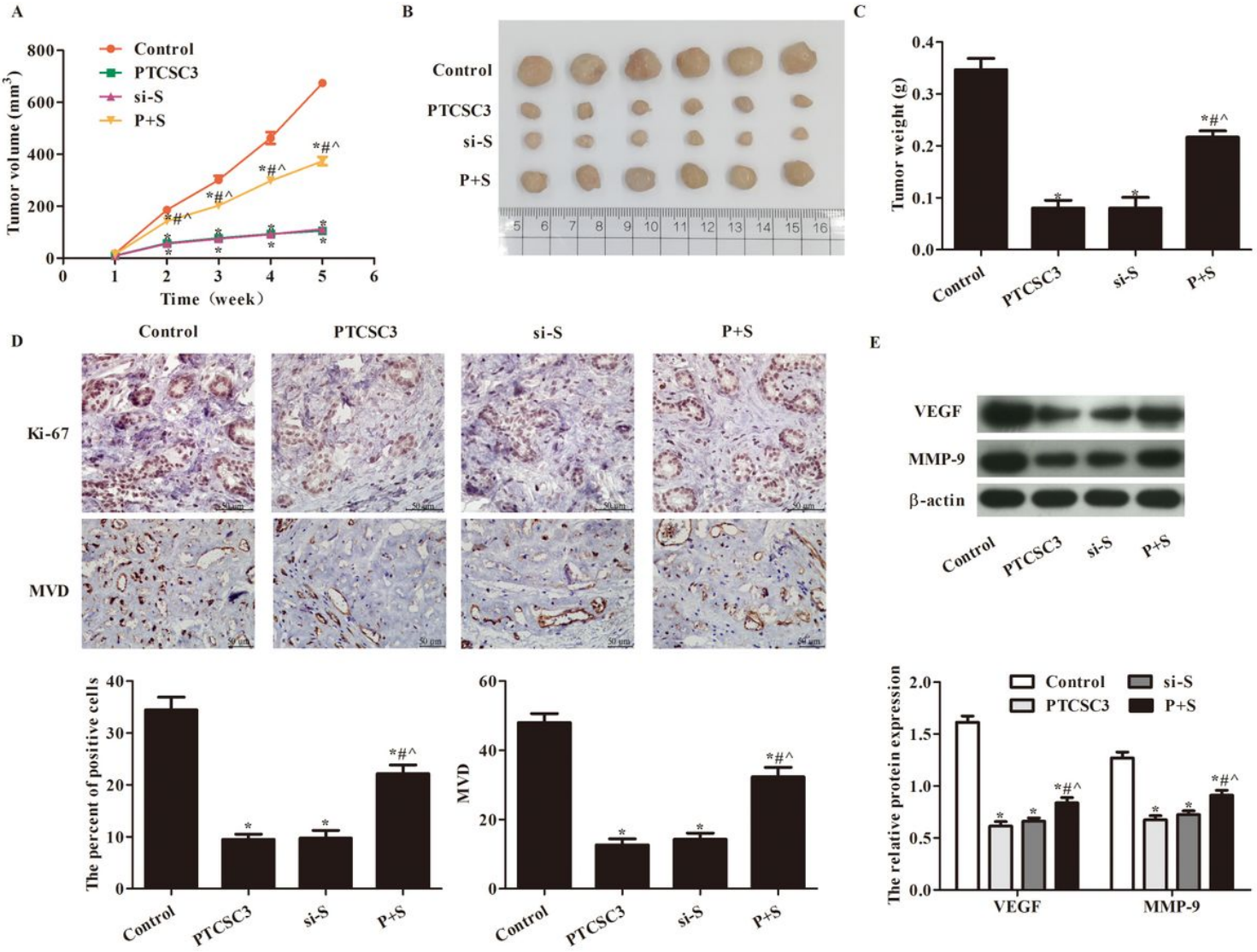

Figure 5

PTCSC3 regulates the effects of S100A4 on tumor growth. (A) tumor volume; (B) tumor photograph; (C) tumor weight; (D) immunohistochemistry to detect Ki67 expression in xenograft tissues (×400); (E) immunohistochemistry to detect tumor microvessel density MVD (× 400); (F) Western blot. Compared to the control group, *p<0.05; compared to PTCSC3, #p<0.05; compared to si-S group, ^ p<0.05. Data analysis results were repeated 3 times and presented as mean±SD. ANOVA was used for data analysis between multiple groups. And Dunnett-t test was used for subsequent analysis.

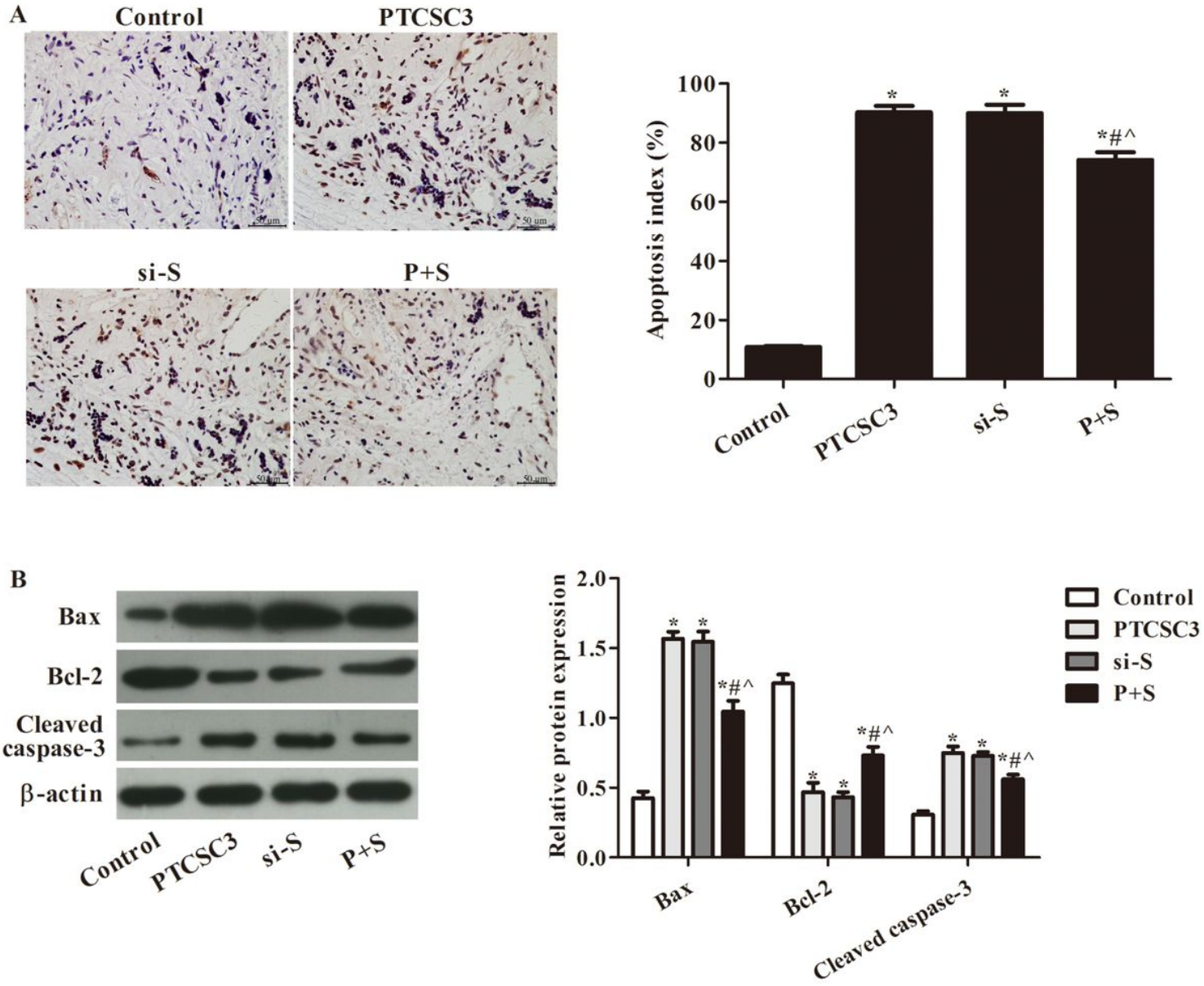

Figure 6

PTCSC3 regulates the effects of S100A4 on tumor apoptosis. (A) TUNEL detected tumor cell apoptosis (×400); (B) Western blot. Compared to the control group, *p<0.05; compared to PTCSC3, #p<0.05; compared to si-S group, ^ p<0.05. Data analysis results were repeated 3 times and presented as mean±SD. ANOVA was used for data analysis between multiple groups. And Dunnett-t test was used for subsequent analysis.